Supporting Information

Equilibration dependence of fucoxanthin S_1 and ICT signatures on polarity, proticity, and temperature by multi-pulse femtosecond absorption spectroscopy

Robert G. West[a], Marcel Fuciman[a], Hristina Staleva-Musto[a], Václav Šebelík[a], David Bína[a,b], Milan Durchan[a,b], Valentyna Kuznetsova[a], Tomáš Polívka[a,b,*]

[a]Faculty of Science, University of South Bohemia, České Budějovice, Czech Republic

[b]Institute of Plant Molecular Biology, Biological Centre, Czech Academy of Sciences, České Budějovice, Czech Republic

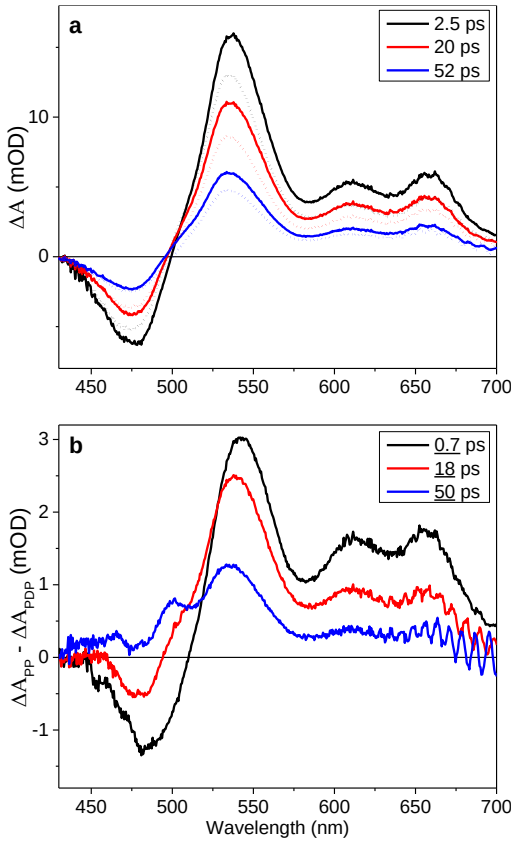

Figure S1. (a) PP (solid) and PDP (dotted) spectra of fucoxanthin in isopropanol at various times after excitation. (b) The double-difference spectrum (PP – PDP) of fucoxanthin in isopropanol. The underlined values indicate the delay time after the dump pulse.

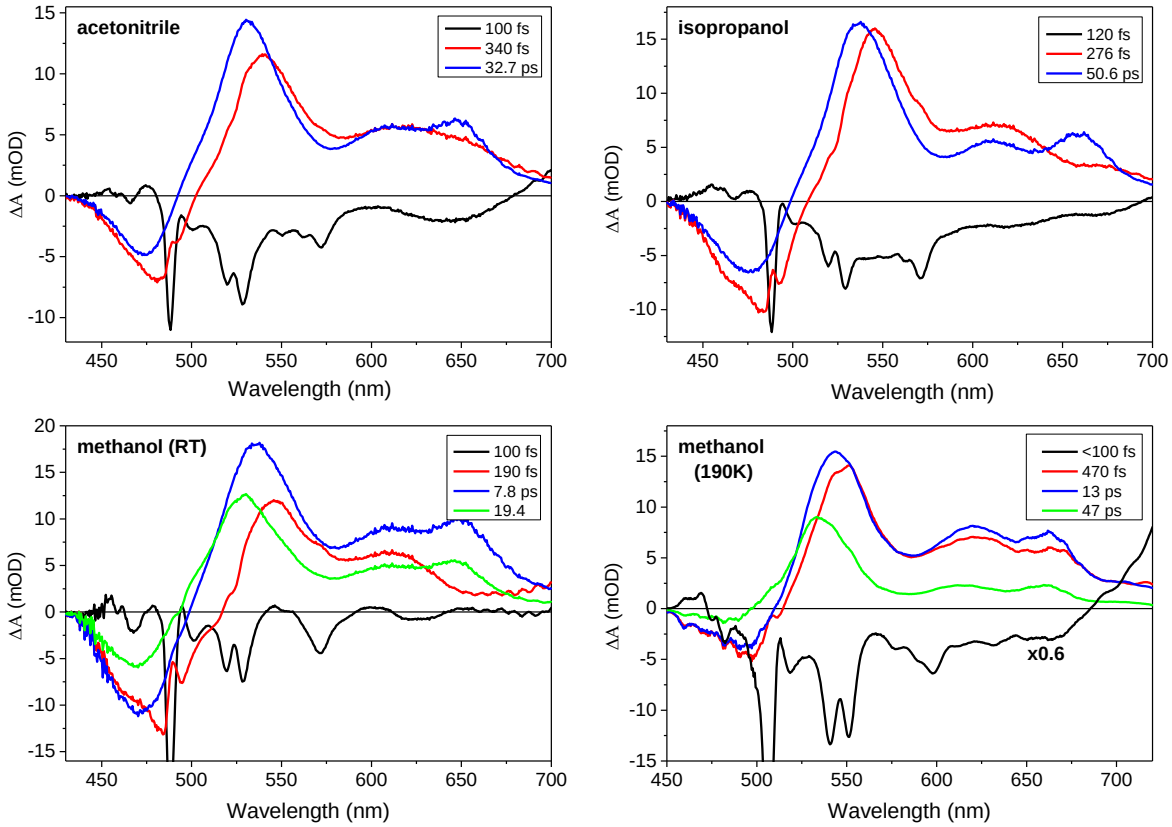

Figure S2. EADS obtained from global fitting the data measured for fucoxanthin in all solvents.

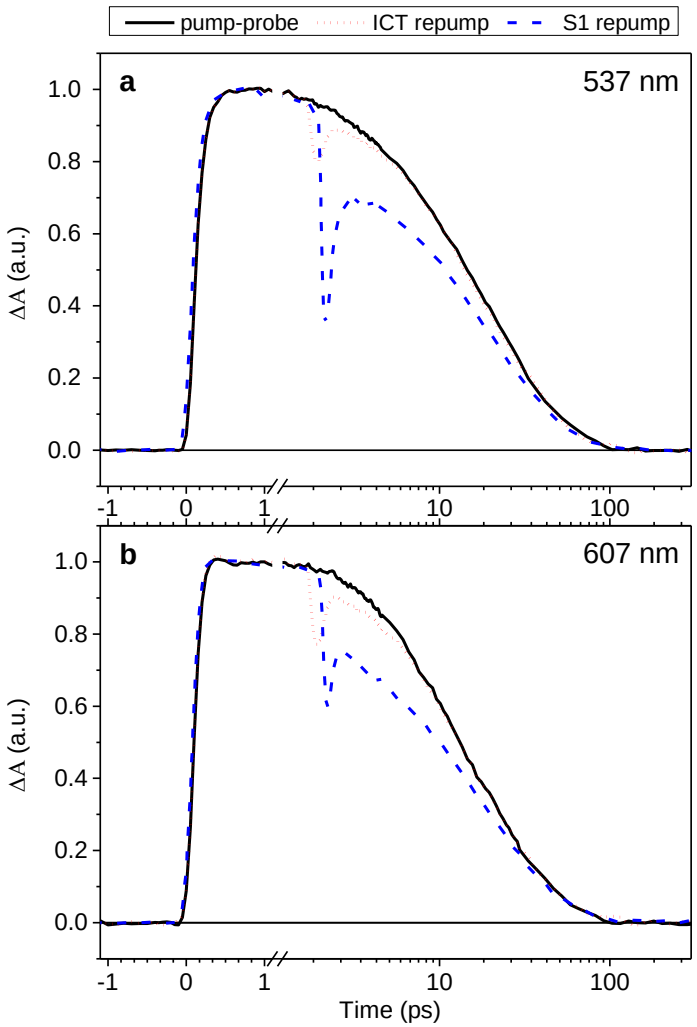

Figure S3. Kinetic traces measured after repumping of either S1 (blue) or ICT (red) state compared to PP traces (black) in (a) the S_1-associated band and (b) the ICT-associated band of fucoxanthin in methanol.

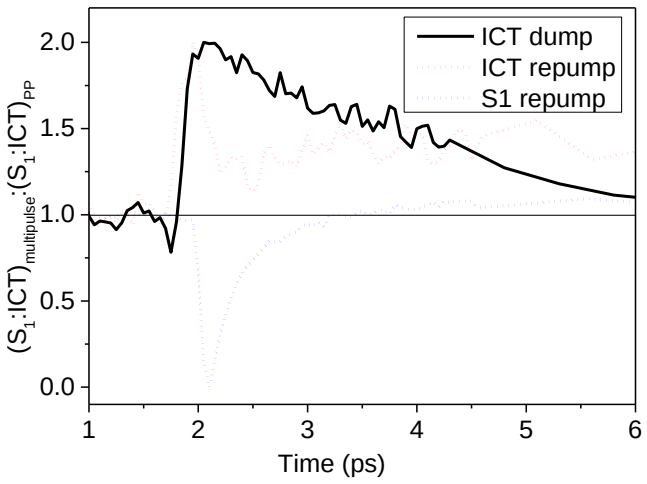

Figure S4. Equlibration dynamics following repumping either the S_1 (blue) or ICT (red) state monitored as amplitude ratio of the S_1-associated and ICT-associated signal normalized to the same signal measured in the PP regime, that is the $(S_1{:}ICT)_{PrPP}{:}(S_1{:}ICT)_{PP}$ ratio. The equilibration dynamics after dumping the ICT state (black) is shown for comparison.

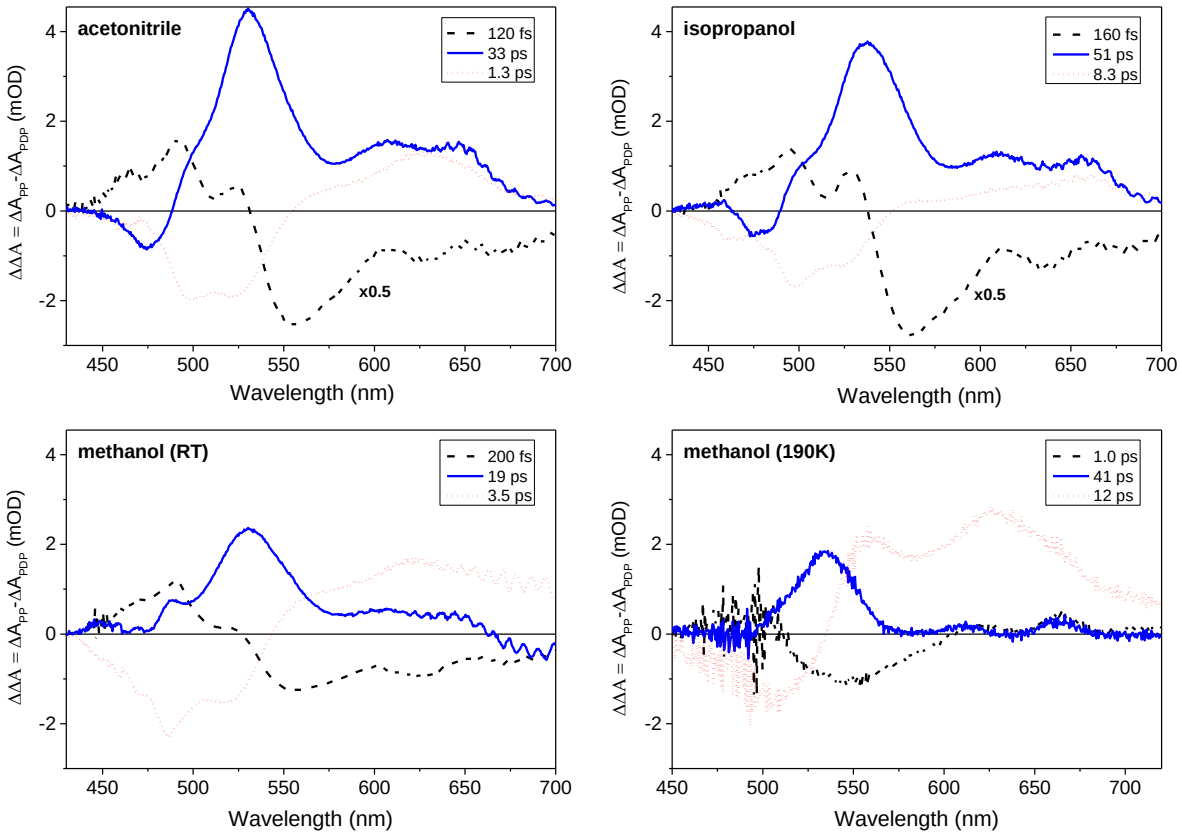

Figure S5. DADS of the double-difference spectrum (PP-PDP) of fucoxanthin in all solvents. The amplitude of the fastest component was reduced by half in each case.

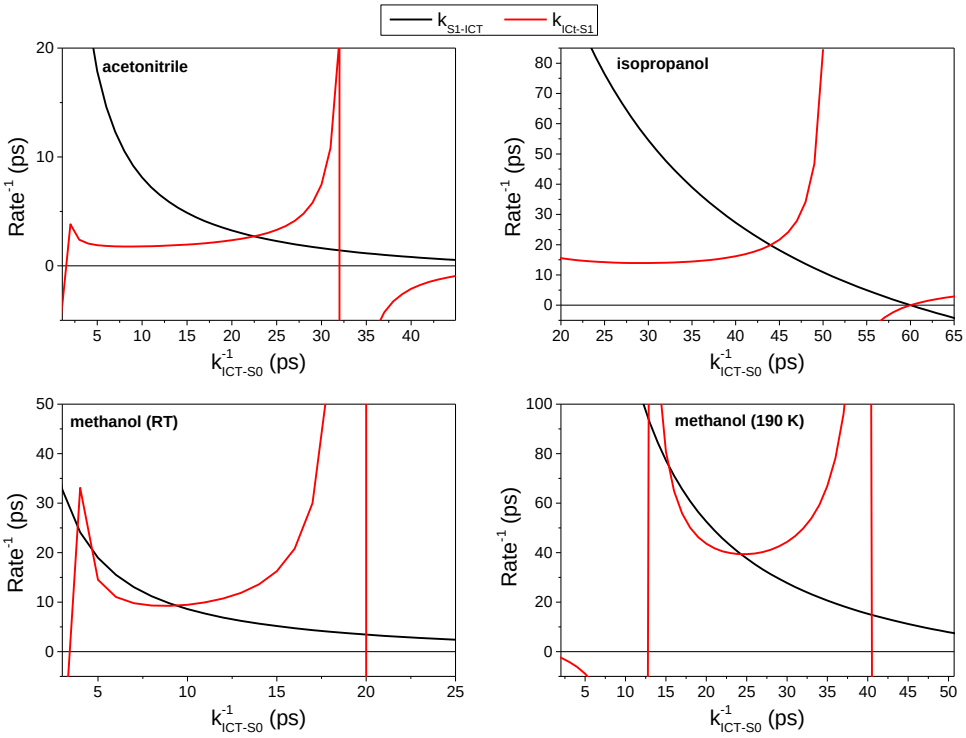

Figure S6. The possible values for the inter-S_1-ICT energy transfer rates $k_{S_1 \to ICT}$ and $k_{ICT \to S_1}$ as a function of ICT-S_0 transfer rate $k_{ICT \to S_0}$ under the two-state model according to the common and equilibrium rates of fucoxanthin in all solvent environments. Curves in methanol at both temperatures are associated with the longer common decay components as found in the EADS.

$(n_{s_1}/n_{ICT})_0$	(S_1/ICT)	(S_1/ICT)$_{PDP}$/ (S_1/ICT)$_{PP}$
0.8	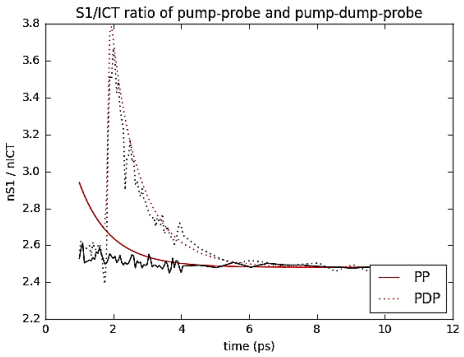	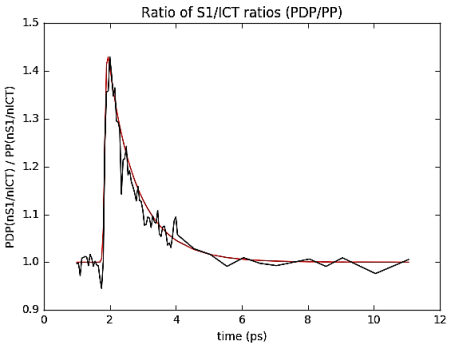
1	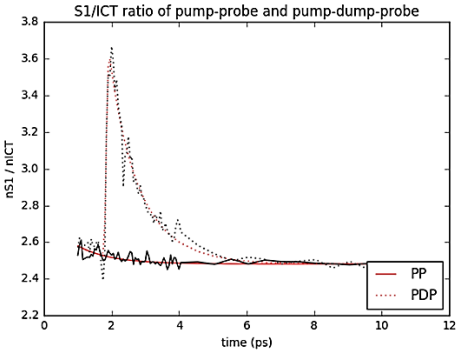	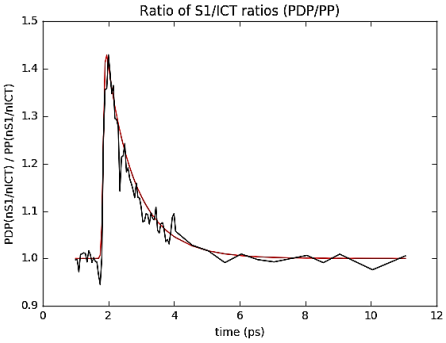
1.2	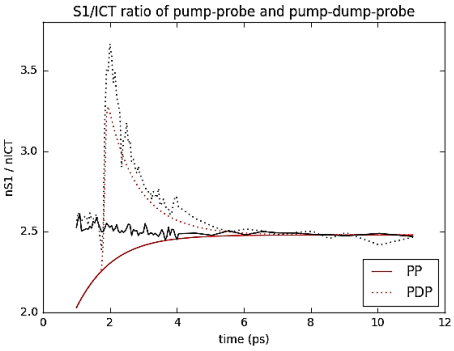	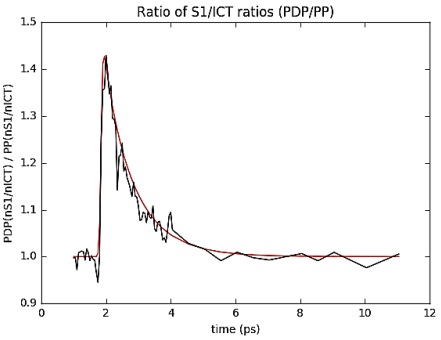

Figure S7. Influence of the initial (at the time of the dumping) population ratio $(n_{S1}/n_{ICT})_0$ on fitting the S_1:ICT ratios of fucoxanthin in acetonitrile.

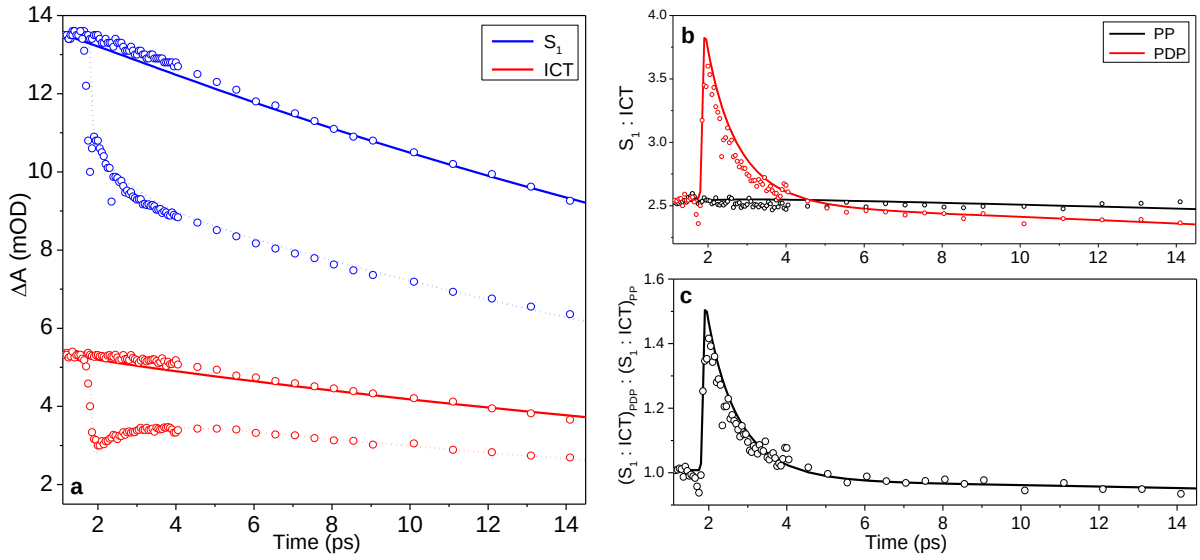

Figure S8. Fits resulting from the two-level model of the coupled S_1 and ICT states for fucoxanthin in acetonitrile. As kinetic signatures of these states and the ground state overlap, the proper amount of S_0 bleaching and excite state absorption (ESA) signal had to be determined in order to match the contributions at 535 nm (61% S_1 ESA, 13% S_0 bleaching, 26% ICT ESA) and 610 nm (91% ICT ESA, 9% S_1 ESA). The dump pulse width is 70 fs, and the rate of dumping is $(120\ \text{fs})^{-1}$. (a) Fits associated with undumped (solid) and dumped (dotted) populations of the S_1 (535 nm) and ICT (610 nm) states. (b) The ratio of the S_1 band to the ICT band (535:610 nm) for undumped (solid) and dumped (dotted) populations. (c) The effect of the dump demonstrated in the ratio of the dumped S_1:ICT ratio (dotted line in b) to the undumped S_1:ICT ratio (solid line in b).